Free Radical Biology and Medicine 243 (2026) 29–42

Contents lists available at ScienceDirect

Free Radical Biology and Medicine

journal homepage: www.elsevier.com/locate/freeradbiomed

Microglial HMOX1 drives retinal angiogenesis via modulation of endothelial STAT3 signaling

Yaling Liu [a], Jiannan Tang [b], Peiling Wei [a], Zhen Yu [a], Zhifei Wu [c], Xinyu Zhao [a], Hui Qi [a], Ping Liu [a], Mianying Zheng [a], Shengli Mi [d], Wei Du [c], Demetrios G. Vavvas [e,*], Kaixuan Cui [a,**], Guoming Zhang [a,***]

[a] Shenzhen Eye Hospital, Shenzhen Eye Medical Center, Southern Medical University, Shenzhen, China
[b] Department of Ophthalmology, The First Affiliated Hospital of Jinan University, Guangzhou, China
[c] Department of Ophthalmology, The Eighth Affiliated Hospital, Sun Yat-Sen University, Shenzhen, China
[d] Bio-manufacturing Engineering Laboratory, Tsinghua Shenzhen International Graduate School, Tsinghua University, Shenzhen, China
[e] Retina Service, Ines and Fred Yeatts Retina Research Laboratory, Angiogenesis Laboratory, Department of Ophthalmology, Harvard Medical School, Massachusetts, Eye and Ear, Boston, MA, USA

ARTICLE INFO

Keywords:
Oxygen-induced retinopathy
Retinal angiogenesis
Microglia
Heme oxygenase-1
STAT3
Endothelial cells

ABSTRACT

Retinopathy of prematurity (ROP) is a leading cause of childhood blindness and is characterized by retinal neovascularization. Microglia have emerged as key mediators of hypoxia-induced angiogenesis, yet the underlying molecular mechanisms remain incompletely defined. Heme oxygenase-1 (HMOX1) is a stress-inducible enzyme with well-established antioxidant and anti-inflammatory properties, acting as an important electrophilic signaling mediator in redox biology. Here, we investigated the role of microglial HMOX1 in retinal angiogenesis and its regulation of endothelial signaling. Using an oxygen-induced retinopathy (OIR) mouse model combined with bulk and single-cell RNA sequencing, we identified HMOX1 as a hypoxia-induced angiogenic regulator selectively enriched in retinal microglia. Conditional knockout of HMOX1 in microglia markedly reduced neovascularization in vivo, while in vitro hypoxia-driven microglia–endothelial co-culture assays confirmed impaired endothelial proliferation, migration, and tube formation. Mechanistically, loss or pharmacological inhibition of HMOX1 suppressed STAT3 activation and VEGF expression in endothelial cells, establishing a paracrine signaling pathway between microglia and endothelium. These findings demonstrate that microglial HMOX1 drives pathological angiogenesis by activating the endothelial STAT3–VEGF axis. Our study uncovers a novel hypoxia–microglia–endothelium signaling mechanism, highlighting microglial HMOX1 as a promising therapeutic target for ROP and other hypoxia-related angiogenic diseases.

1. Introduction

Retinopathy of prematurity (ROP) is a developmental retinal vasculopathy characterized by retinal neovascularization secondary to disrupted neurovascular maturation, and it remains one of the leading preventable causes of childhood blindness worldwide [1,2]. The pathogenesis of ROP involves two phases [3]: phase I, where premature birth halts retinal vascular development, causing relative hypoxia as the retina matures; and phase II, where hypoxia upregulates oxygen-sensitive factors like erythropoietin and vascular endothelial growth factor (VEGF), driving neovascularization. Currently, laser photocoagulation and intravitreal anti-VEGF therapies are the mainstays of treatment during phase II. However, both interventions have notable limitations [4], particularly concerning anti-VEGF therapy, as systemic suppression of VEGF following intravitreal administration raises concerns about potential long-term ocular and systemic developmental complications [5]. Given these limitations, there is an urgent need to deepen our understanding of the molecular mechanisms

* Corresponding author. Retina Service, Ines and Fred Yeatts Retina Research Laboratory, Angiogenesis Laboratory, Department of Ophthalmology, Massachusetts Eye and Ear, Harvard Medical School, Boston, MA, 02114, USA.
** Corresponding author. Shenzhen Eye Hospital, Shenzhen Eye Medical Center, Southern Medical University, Shenzhen, 518040, China.
*** Corresponding author. Shenzhen Eye Hospital, Shenzhen Eye Medical Center, Southern Medical University, Shenzhen, 518040, China.
E-mail addresses: demetrios_vavvas@meei.harvard.edu (D.G. Vavvas), cuikxeye@163.com (K. Cui), 13823509060@163.com (G. Zhang).

https://doi.org/10.1016/j.freeradbiomed.2025.11.018
Received 19 October 2025; Received in revised form 9 November 2025; Accepted 10 November 2025
Available online 11 November 2025
0891-5849/© 2025 Elsevier Inc. All rights are reserved, including those for text and data mining, AI training, and similar technologies.

underlying neovascularization in ROP and to identify novel therapeutic targets to optimize outcomes and minimize adverse effects.

Microglia, the resident immune cells of the central nervous system, play a critical role in regulating developmental retinal angiogenesis and actively contribute to neovascularization under disease conditions [6]. In the oxygen-induced retinopathy (OIR) model, microglia become activated and migrate toward hypoxic regions, where they are thought to modulate the vascular microenvironment [7]. Recent single-cell transcriptomic studies have revealed that microglia contribute to neovascularization in retinal vascular diseases [6,8,9]. In contrast, in other regions of the central nervous system, microglia have been shown to promote endothelial wound healing, suggesting a beneficial role in vascular repair [10]. These findings indicate that the interaction between microglia and endothelial cells (ECs) may vary across different pathological conditions. In the OIR retina, however, the specific roles and mechanisms by which microglia influence endothelial behavior remain poorly understood and require further investigation.

Heme oxygenase-1 (HMOX1) is a classic stress-inducible enzyme that is upregulated under pathological conditions such as hypoxia and inflammation [11]. It exerts a variety of biological effects, including antioxidant, anti-inflammatory, and anti-proliferative functions [12]. HMOX1 has been closely linked to angiogenesis in various diseases, and previous studies have demonstrated that it can promote neovascularization by regulating the expression of VEGF [13–16]. Despite the established relationship between HMOX1 and VEGF, its specific role in retinal neovascularization, particularly its function within microglia, remains poorly understood. Investigating the HMOX1-mediated regulatory mechanisms in microglia may provide new insights into its pathogenic roles in diseases such as ROP.

In this study, we employed bulk RNA sequencing and single-cell RNA sequencing analyses, in combination with a human microglial cell line (HMC3), human retinal microvascular endothelial cells (HRMVECs), and the OIR mouse model, to investigate the role of microglial HMOX1 in retinal neovascularization. We found that HMOX1 expression was specifically upregulated in microglia from OIR retinas, with expression levels correlating positively with the severity of neovascular lesions. Genetic ablation of HMOX1 in microglia using Cx3cr1 promoter-driven Cre recombinase (Cx3cr1-Cre) in conditional knockout mice, as well as pharmacological inhibition of HMOX1 in vitro, both led to reduced neovascularization and attenuated endothelial cell proliferation. These effects were accompanied by decreased expression of endothelial activator of transcription 3 (STAT3) and VEGF in both in vivo and in vitro settings. Collectively, these findings reveal a previously unrecognized role of microglial HMOX1 in retinal neovascularization and suggest that HMOX1 may serve as a potential therapeutic target for angiogenic retinal diseases, including ROP.

2. Material and methods

2.1. Animals

All animals were housed in a specific pathogen-free facility at TOP-BIOTECH (Shenzhen, China). All experimental procedures were approved by the Ethics Committee of Shenzhen Eye Medical Center, Southern Medical University (Approval No. D2307020), and conducted in accordance with the ARVO Statement for the Use of Animals in Ophthalmic and Vision Research.

2.2. Induction of OIR model

Newborn C57BL/6J mice (postnatal day 0, P0) were exposed to 75 ± 2 % oxygen from P7 to P12 in an airtight chamber (Huaxiao Electronics, Changsha, China) with an oxygen flow rate of 0.50–0.75 L/min. Subsequently, the mice were returned to room air until P17. During hyperoxia, pups were reared by alternating foster dams, and body weight as well as general health were monitored at P7, P12, and P17 [17,18]. Pups showing poor health or markedly reduced growth were excluded in accordance with predefined humane endpoints. *n* indicates the number of eyes analyzed unless otherwise specified; both eyes from each animal were included. Group sizes are reported in each figure legend. Retinal tissues were collected at designated time points for subsequent analyses.

2.3. Generation and induction of microglia-specific HMOX1 conditional knockout mice

$HMOX1^{flox/+}$; Cx3cr1-$CreERT2^{+/-}$ mice were purchased from Cyagen Biosciences Inc (Suzhou, Jiangsu, China) and intercrossed to generate $HMOX1^{flox/flox}$; Cx3cr1-$CreERT2^{+/-}$ (HMOX1 cKO) mice and $HMOX1^{flox/flox}$ littermates as controls. Tamoxifen (Sigma-Aldrich, St. Louis, MO, USA) was intraperitoneally injected at 20 mg/kg daily for five consecutive days starting at P12 to induce Cre-mediated recombination. Genotyping was performed to confirm knockout efficiency.

2.4. Bulk RNA sequencing and single-cell RNA sequencing (scRNA-seq)

For bulk RNA-seq (Gene Denovo Biotechnology Co., Ltd., Guangzhou, China), total RNA was extracted from retinal tissues, and mRNA was enriched using Oligo (dT) beads. After fragmentation and reverse transcription, cDNA libraries were constructed and sequenced using an Illumina platform. RNA quality was assessed via agarose gel electrophoresis, NanoPhotometer, Qubit 2.0, and Agilent 2100.

For scRNA-seq, retinal tissues were enzymatically dissociated into single-cell suspensions. Cells with >90 % viability were processed using the 10x Genomics Chromium system and Single Cell 3′ Reagent Kits v3 (Gene Denovo Biotechnology Co., Ltd., Guangzhou, China). Sequencing was performed on an Illumina platform, and data were processed with Cell Ranger (v3.0, mm10 reference genome) and analyzed using Seurat (v3.0) in R.

2.5. Cell culture and co-culture experiments

Human microglial HMC3 cells (Yuchi Biotechnology Co., Ltd., Shanghai, China) were cultured in DMEM supplemented with 10 % fetal bovine serum (FBS; Gibco, Waltham, MA, USA) and 1 % penicillin/streptomycin at 37 °C in 5 % CO_2. Human retinal microvascular endothelial cells (HRMVECs; Fenghbio, China) were cultured in Complete Classic Medium with serum and supplements. For co-culture, HMC3 cells were pretreated under normoxic or hypoxic (1 % O_2) conditions with or without zinc protoporphyrin IX (ZnPP, 10 μM), then co-cultured with HRMVECs in Transwell systems for 24 h.

2.6. Intravitreal injection of HMOX1 inhibitor

At P12, OIR mice received intravitreal injections of ZnPP (20 μM in 1 μL; Sigma-Aldrich, St. Louis, MO, USA) into the right eye. The contralateral eye was injected with 1 μL of PBS as a control. Retinas were harvested at P17 for wholemount staining and analysis of neovascular and avascular areas.

2.7. Quantification of retinal neovascularization

At P17, eyes were enucleated and fixed in 4 % paraformaldehyde (PFA) for 30 min. Retinas were dissected and incubated overnight at 4 °C with Alexa Fluor 594-conjugated Isolectin B4 (IB4; Invitrogen, USA). After washing, retinas were incised radially into four quadrants and flat-mounted with the photoreceptor side down. Imaging was performed using a confocal microscope (Nikon A1R, Tokyo, Japan). Neovascular tufts and avascular areas were quantified using ImageJ software and expressed as a percentage of total retinal area.

2.8. Quantitative PCR (qPCR)

Total RNA was extracted from HMC3 cells or retinal tissue using TRIzol reagent (TransGen Biotech, China). First-strand cDNA synthesis was performed using a qPCR RT Master Mix (TransGen Biotech, China). qPCR was carried out with SYBR Green Master Mix (Invitrogen, USA) on an ABI Prism 7500 Real-Time PCR System (Applied Biosystems, USA). β-actin was used as the internal control. Primer sequences are listed (Table S1). All reactions were performed in triplicate.

2.9. Western blotting

Protein lysates from retinal tissues and cultured cells were prepared using RIPA lysis buffer (Beyotime, China) supplemented with protease and phosphatase inhibitor tablets (Thermo Fisher Scientific, USA). Protein concentrations were measured using the BCA Protein Assay Kit (Thermo Fisher Scientific, USA). Equal amounts of protein (30 μg per sample) were separated by 8–12 % SDS-PAGE and transferred onto PVDF membranes (EpiZyme, USA). Membranes were blocked with 5 % non-fat milk at room temperature for 1 h and then incubated overnight at 4 °C with primary antibodies, followed by appropriate HRP-conjugated secondary antibodies. Signals were visualized using enhanced chemiluminescence (ECL) detection reagents (Beyotime, China) and quantified using ImageJ software.

As shown in Table S2, primary antibodies were used: anti-HMOX1 (Proteintech, Wuhan, China), anti-Iba1 (R&D Systems, Minneapolis, MN, USA), anti-STAT3 and anti-phospho-STAT3 (pSTAT3, SAB Biotech, Maryland, USA), anti-CD31 (Abcam, Cambridge, UK), anti-VEGFA (Abclonal Technology, Wuhan, China), and anti-β-actin (Abcam, Cambridge, UK).

2.10. Immunofluorescence staining

Eyeballs were fixed in 4 % PFA, dehydrated in a sucrose gradient, embedded in OCT (Sakura Finetek, USA), and cryosectioned at 8 μm. Sections were incubated with primary antibodies overnight at 4 °C, followed by fluorescent secondary antibodies. For wholemount staining, retinas were flat-mounted after antibody incubation. Cultured cells were fixed, permeabilized, blocked, and stained similarly.

As shown in Table S2, primary antibodies included anti-HMOX1, anti-Iba1, anti-STAT3, IB4, and anti-CD31. Secondary antibodies included Alexa Fluor 488-, 594-, or 647-conjugated IgG antibodies (Abcam and CST). Images were acquired using a confocal microscope (Nikon A1R, Tokyo, Japan).

2.11. Hematoxylin and eosin (H&E) staining

Eyes were fixed in 4 % formaldehyde overnight, embedded in paraffin, and sectioned vertically at 5 μm thickness. After deparaffinization and rehydration, sections were stained with hematoxylin for 10 min, rinsed, and counterstained with eosin for 15 s. Sections were dehydrated, cleared, and mounted. Neovascular nuclei anterior to the inner limiting membrane and retinal thickness were quantified under a light microscope.

2.12. Optical coherence tomography (OCT)

Mice were anesthetized via intraperitoneal injection of tribromoethanol (20 ml/kg, AibeiBio, Nanjing, China). Pupils were dilated with 1 % tropicamide, and Genteal gel (Alcon) was applied to prevent corneal dehydration. Retinal imaging was performed using the Micron IV system (Phoenix Research Labs), with fundus photography for initial alignment and real-time OCT images for fine adjustment. Cross-sectional retinal images were acquired for morphological analysis.

2.13. Fundus fluorescein angiography (FFA)

Following OCT, FFA was conducted using the same system. After pupil dilation and ocular surface cleaning, 0.01 ml of 25 % sodium fluorescein (Akorn Inc) per 5 g body weight was injected intraperitoneally. Retinal vessels were visualized within 1 min post-injection. Images were captured at 1 and 5 min to evaluate vascular perfusion and leakage.

2.14. Cell viability assay using 3-(4,5-dimethylthiazol-2-yl)-2,5-diphenyl tetrazolium bromide (MTT)

Cells were seeded in 96-well plates (5×10^3 cells/well) and incubated for 12 h. After treatment, 20 μl of MTT solution (5 mg/ml in PBS, Sigma-Aldrich) was added per well and incubated at 37 °C for 4 h. Supernatants were removed, and 150 μl of DMSO was added to dissolve formazan crystals. Absorbance at 490 nm was measured using a microplate reader (Bio-Rad, Hercules, CA, USA).

2.15. 5-ethynyl-2′-deoxyuridine (EdU) incorporation assay

Endothelial cell proliferation was evaluated using a Click-iT™ EdU Imaging Kit (Beyotime, China). HRMVECs were seeded in the lower chamber and HMC3 microglia in the upper insert of a 6-well Transwell (Corning #3450). After 24 h co-culture under normoxia or hypoxia with/without ZnPP, EdU was added for 2 h. Cells were fixed, stained per protocol, and imaged using a Nikon confocal microscope.

2.16. Wound healing assay

HRMVECs were cultured to confluence in 6-well Transwell plates. A scratch was made with a pipette tip, followed by co-culture with HMC3 cells in the upper chamber. After 24 h under combinations of ZnPP treatment (±ZnPP) and oxygen levels (normoxia/hypoxia), images were taken at 0 and 24 h. Wound closure was quantified using ImageJ.

2.17. Transwell migration assay

Endothelial migration was assessed using 24-well Transwell inserts (8 μm pores; Corning #3470). HMC3 cells were seeded in the lower wells and HRMVECs (2×10^4/ml) in the upper chamber. After 24 h co-culture under indicated conditions (with/without ZnPP, normoxia/hypoxia), migrated cells were fixed, stained with crystal violet, and counted in three random fields per well.

2.18. Tube formation assay

HRMVECs (2×10^4/well) were seeded on Matrigel-coated 24-well plates (Corning #354234) and co-cultured with HMC3 cells in the upper chamber. After 24 h incubation (with/without ZnPP, normoxia/hypoxia), tube-like structures were imaged in three fields using a Leica microscope and quantified with ImageJ.

2.19. Statistical analysis

Data are presented as mean ± standard deviation (SD). Comparisons between two groups were performed using the unpaired two-tailed Student's t-test or Mann–Whitney *U* test, as appropriate. For comparisons among three or more groups, one-way analysis of variance (ANOVA) followed by Bonferroni post hoc test was used. All analyses were performed using SPSS v27.0 software (IBM, Chicago, IL, USA). A P value < 0.05 was considered statistically significant (*$p < 0.05$; **$p < 0.01$; ***$p < 0.001$; ****$p < 0.0001$).

3. Results

3.1. HMOX1 is progressively upregulated during retinal neovascularization

To validate the successful establishment of the OIR model, we first performed retinal flat-mount fluorescein angiography at P17. Distinctive avascular and neovascular zones were clearly observed (Fig. S1A), and quantitative analysis confirmed consistent changes in area size (Fig. S1B and C), supporting the model's reliability [17]. Given the well-characterized temporal progression of angiogenesis in OIR [17], bulk RNA-seq was conducted on retinal tissues harvested at P12, P13, and P17 from OIR mice, and at P17 from age-matched controls. Differential gene expression analysis revealed substantial transcriptional alterations across the time points (Fig. 1A), with numerous genes significantly upregulated or downregulated (Fig. 1B), providing a foundation for downstream analyses. Among these, HMOX1 expression was markedly increased in OIR retinas and showed a progressive elevation that paralleled the severity of neovascularization (Fig. 1C and D). Quantitative expression profiling confirmed this trend (Fig. 1E). Gene Ontology (GO) and Kyoto Encyclopedia of Genes and Genomes (KEGG) enrichment analyses revealed that differentially expressed genes were significantly associated with angiogenesis-related pathways, including ferroptosis signaling (Fig. 1F and G). Additionally, protein–-protein interaction (PPI) network analysis suggested that HMOX1 may interact directly with VEGF or indirectly through STAT3 (Fig. 1H). Collectively, these results indicate that HMOX1 is progressively upregulated in the OIR retina and may contribute to angiogenesis via the STAT3–VEGF signaling axis.

3.2. Microglial HMOX1 is upregulated and linked to endothelial STAT3–VEGF signaling

To delineate the cellular distribution of HMOX1 during neovascularization, we performed scRNA-seq on retinas from OIR mice using the 10x Genomics platform (Fig. 2A and B). Quality control metrics confirmed the robustness of the data (Fig. S1D–G). To enhance immune cell resolution, rod photoreceptors were depleted using magnetic bead-based sorting prior to sequencing [8]. Clustering analysis identified 11 distinct retinal cell populations (Fig. 2C), with microglia significantly enriched in OIR compared to controls (Fig. 2D). Uniform Manifold Approximation and Projection (UMAP) visualization showed that HMOX1 was broadly expressed across retinal cell types, most prominently in microglia (Fig. 2E and F). Volcano plot analysis further confirmed HMOX1 upregulation in OIR-associated microglia (Fig. 2G). GO enrichment analysis of upregulated genes in microglia revealed strong associations with hypoxia response and cell migration (Fig. 2H). Notably, downregulated genes were also enriched in pathways related to morphogenesis and differentiation (Fig. S1H), suggesting a dual regulatory effect of hypoxia on microglial functional states. PPI analysis indicated potential interactions between HMOX1 and key pro-angiogenic regulators such as STAT3 (Fig. 2I). Cell communication network analysis further revealed strong microglia–endothelial crosstalk mediated by VEGF-related ligand–receptor interactions (Fig. 2J). These results suggest that microglial HMOX1 may contribute to neovascularization in OIR through modulation of endothelial STAT3–VEGF signaling.

3.3. HMOX1 is upregulated in microglia and linked to retinal neovascularization

To validate the microglial specificity of HMOX1 observed in scRNA-seq, immunofluorescence staining was performed on retinal sections and flat mounts. Co-localization analysis revealed that HMOX1 exhibited strong spatial overlap with Iba1$^+$ microglia, and partial overlap with IB4$^+$ endothelial cells, indicating that HMOX1 is predominantly expressed in microglia, while also present in regions adjacent to neovascular tufts in the OIR retina (Fig. 3A and D). Quantitative analysis showed a significant increase in both Iba1$^+$ microglia and IB4$^+$ endothelial cells in OIR retinas compared to controls (Fig. 3B and C), supporting a potential role of microglial HMOX1 in pathological angiogenesis.

Given the distinct temporal phases of neovascularization in the OIR model, retinal tissues from OIR and control mice were collected at multiple time points (P7, P12, P13, P15, P17, P21, and P25) to assess the dynamic expression pattern of HMOX1 [17]. Western blot analysis revealed a time-dependent increase in HMOX1 expression in the OIR retina, peaking at P17 (Fig. 3F and G). This trend was further corroborated by qPCR analysis showing a similar temporal expression pattern (Fig. 3E), indicating a strong correlation between HMOX1 expression and the angiogenic phase of the OIR model.

To examine the regulation of HMOX1 under hypoxia, HMC3 microglial cells were exposed to 1 % O_2 for 12, 24, and 48 h. Both qPCR and Western blot analyses demonstrated time-dependent upregulation of HMOX1 (Fig. 3H–J). Immunofluorescence further confirmed HMOX1 induction in Iba1$^+$ cells under hypoxia (Fig. 3K and L). To explore functional involvement of HMOX1 in angiogenesis, OIR mice received intravitreal injections of the HMOX1 inhibitor ZnPP. Although the avascular area remained unchanged, ZnPP treatment significantly reduced neovascularization (Fig. S2A–C), supporting a role for microglial HMOX1 in promoting retinal angiogenesis.

3.4. Microglia-specific deletion of HMOX1 reduces retinal neovascularization in OIR mice

To assess the impact of microglial HMOX1 on retinal neovascularization, microglia-specific conditional knockout (HMOX1 cKO) mice were generated (Fig. 4A and S3A). Western blot analysis confirmed a significant reduction of HMOX1 protein levels in the retinas of cKO mice compared to Hmox1$^{fl/fl}$ controls in the OIR model (Fig. 4B and C). Immunofluorescence staining revealed a reduction of HMOX1 expression in Iba1$^+$ microglia, which was accompanied by a decrease in IB4$^+$ endothelial cells in the OIR-cKO group (Fig. 4D). Quantification showed a significant decrease in HMOX1$^+$ cells and microglia number in OIR-cKO retinas (Fig. 4E and G), along with a reduced neovascular area (Fig. 4F). These results indicate that microglial HMOX1 deletion mitigates retinal neovascularization in the OIR model.

At P17, fundus imaging and OCT demonstrated more organized retinal structure and normalized total and inner retinal thickness in OIR-cKO mice compared to OIR-Hmox1$^{fl/fl}$ controls (Fig. 4H–J). Whole-mount IB4 staining further showed reduced neovascular and avascular areas in OIR-cKO retinas (Fig. 4K–M). No significant differences were observed between CON-Hmox1$^{fl/fl}$ and CON-cKO groups.

Serial FFA and OCT imaging at P12, P17, P21, and P25 demonstrated that OIR-cKO mice consistently exhibited smaller avascular and neovascular areas, along with relatively preserved retinal thickness compared to OIR- Hmox1$^{fl/fl}$ mice (Figs. S4A and S5A–C). Retinal thickness in OIR-cKO mice was transiently reduced before P21 but normalized by P25. H&E staining at P17 showed reduced preretinal neovascular nuclei and preserved retinal layer structure in OIR-cKO mice (Fig. 4N–P). No structural abnormalities were observed between CON-Hmox1$^{fl/fl}$ and CON-cKO groups, whereas significant pathological attenuation was evident in OIR-cKO retinas (Fig. S5D–E). Collectively, these findings support a critical role for microglial HMOX1 in promoting retinal neovascularization, and demonstrate that its specific ablation alleviates ischemia-induced retinal pathology.

3.5. Microglial HMOX1 promotes endothelial angiogenic behavior in vitro

To examine the functional contribution of microglial HMOX1 to angiogenesis, we established an in vitro co-culture system comprising HMC3 microglia and HRMVECs under hypoxic conditions. Due to

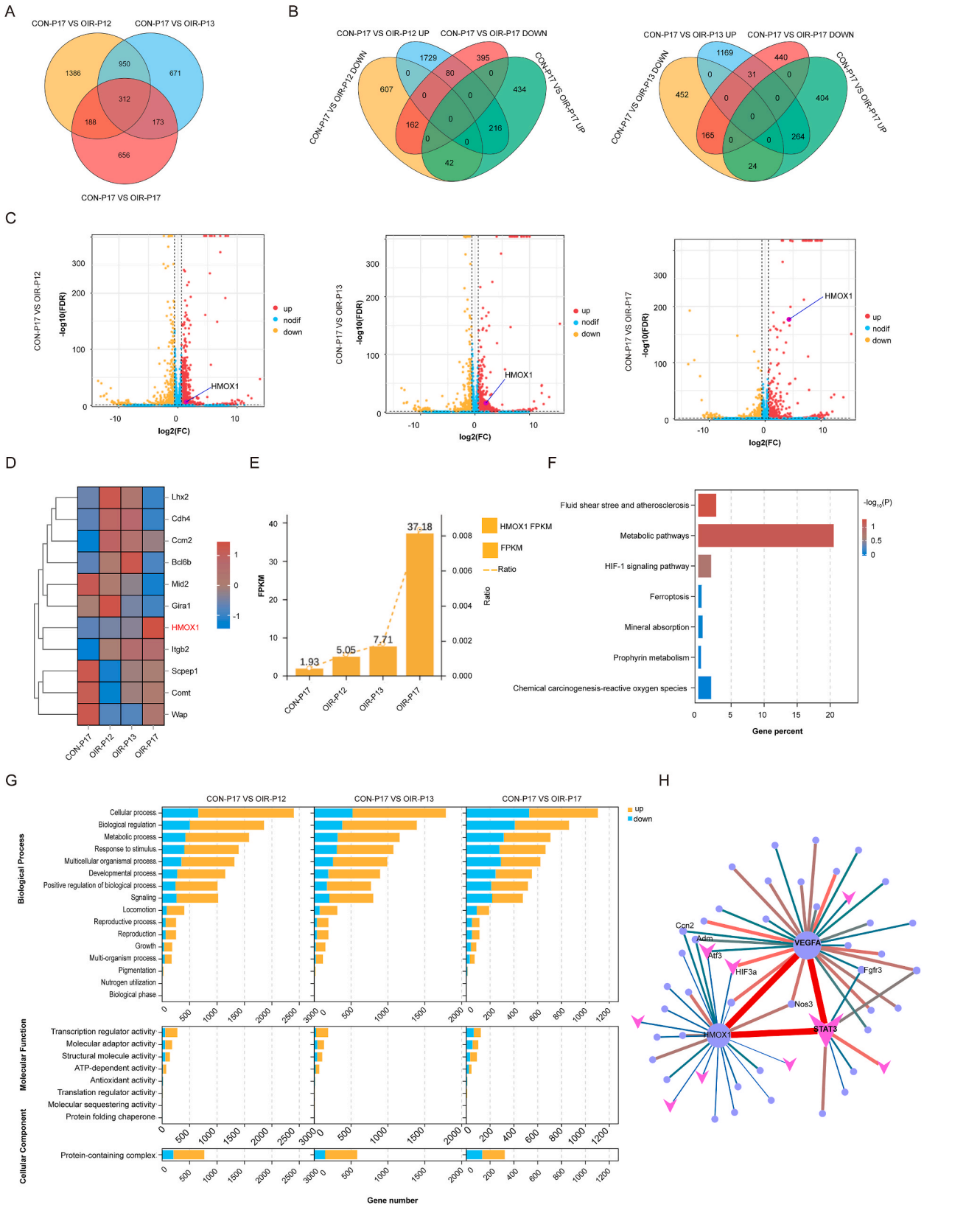


Fig. 1. Bulk RNA-seq analysis reveals elevated expression of HMOX1 in OIR. **(A)** Venn diagram showing the overlap of differentially expressed genes (DEGs) among CON-P17 and OIR-P12, OIR-P13, and OIR-P17. **(B)** Venn diagrams showing the number of upregulated and downregulated genes between CON-P17 and each OIR group. **(C)** Volcano plots illustrating differential expression, highlighting HMOX1 upregulation in OIR-P12, OIR-P13, and OIR-P17 versus CON-P17. **(D)** Heatmap displaying expression patterns of representative DEGs across all groups. **(E)** Bar graphs showing relative expression levels of HMOX1 in the indicated groups. **(F)** KEGG pathway enrichment analysis of DEGs. **(G)** GO enrichment analysis of DEGs. **(H)** PPI network analysis identifying candidate genes potentially interacting with HMOX1.

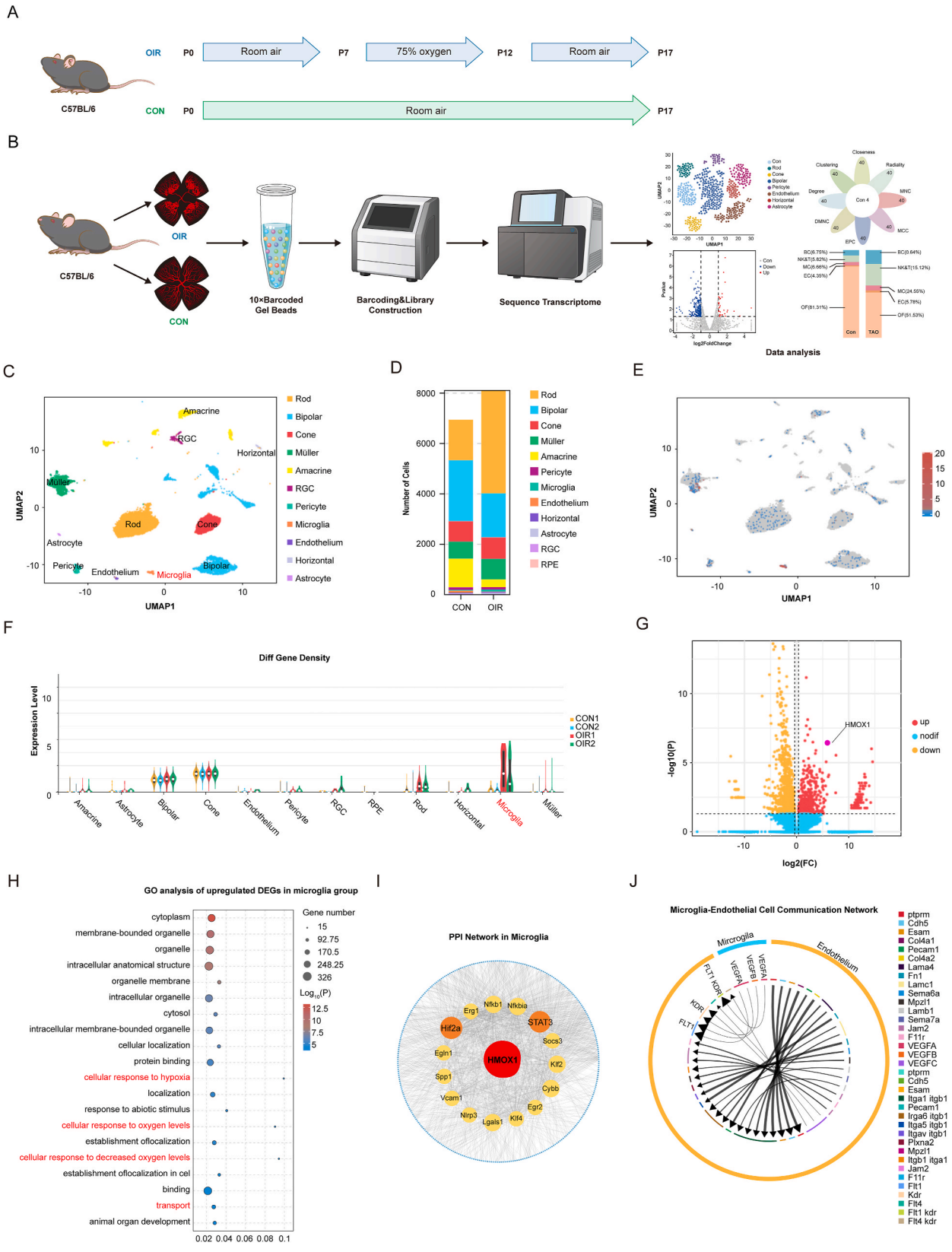


Fig. 2. Microglial HMOX1 is upregulated and linked to endothelial STAT3–VEGF signaling. **(A)** Schematic illustration of the OIR model. **(B)** Workflow diagram of scRNA-seq. **(C)** UMAP plot showing major retinal cell populations. **(D)** Bar graph indicating the relative proportions of each major cell type in CON and OIR groups. **(E)** UMAP heatmap showing the expression distribution of HMOX1 across different cell clusters. **(F)** Violin plots showing HMOX1 expression in each cell cluster between CON and OIR retinas. **(G)** Volcano plot highlighting differential expression of HMOX1 in retinal microglia between OIR and CON groups. **(H)** GO enrichment analysis of upregulated DEGs in microglial group. **(I)** PPI network of potential HMOX1-interacting partners in microglia. **(J)** Cell communication network analysis indicating potential interaction between microglia and endothelial cells.

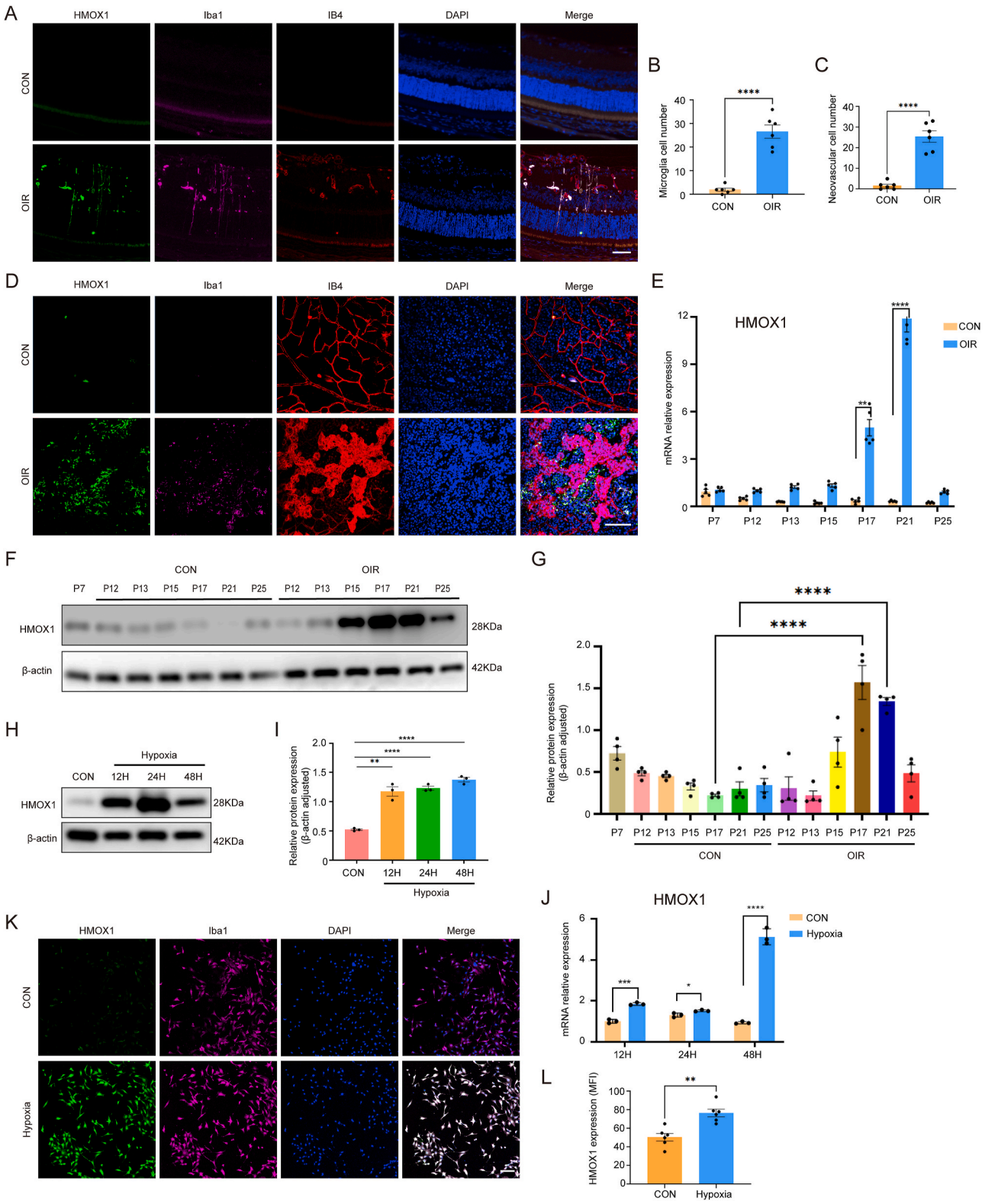
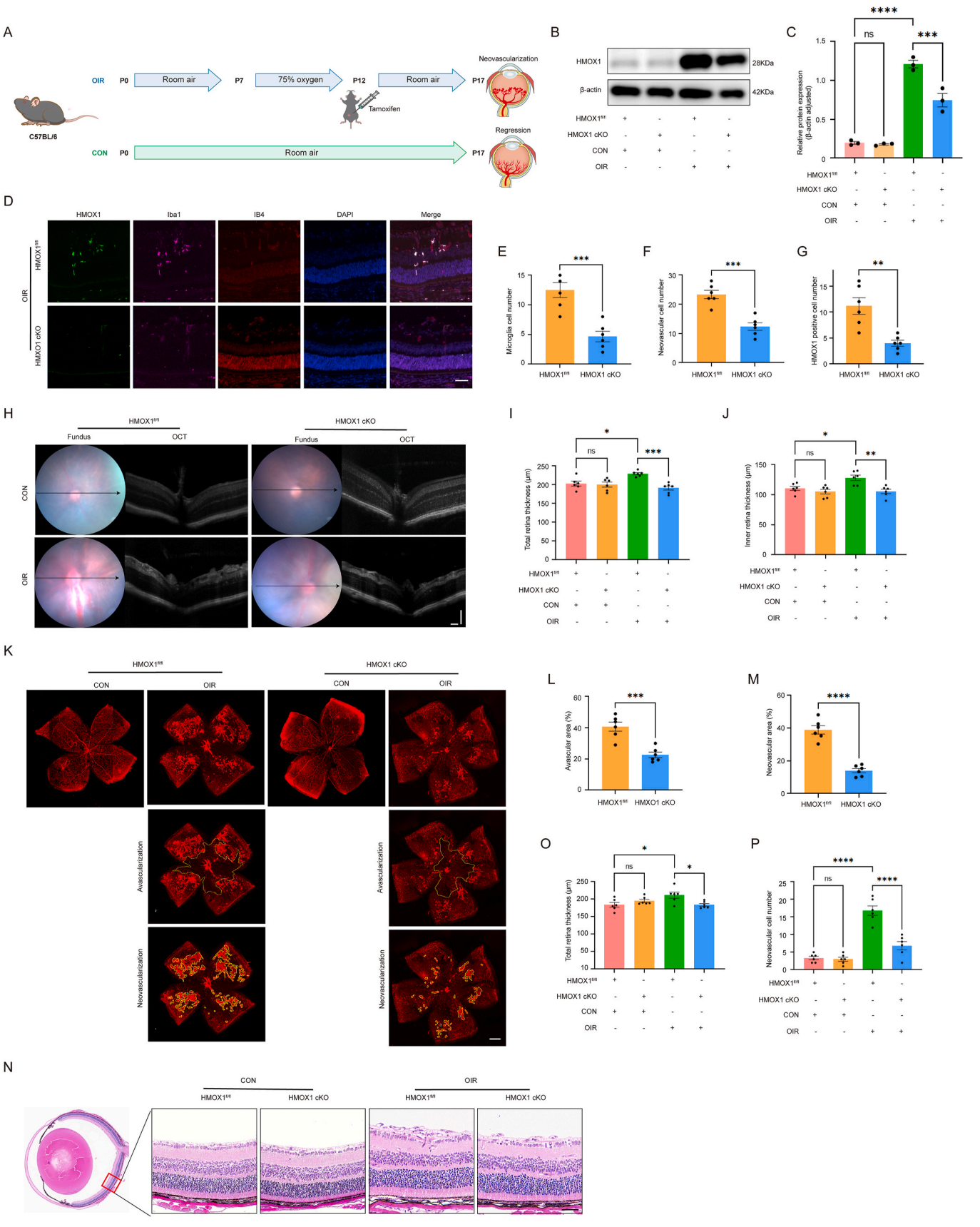


Fig. 3. HMOX1 is upregulated in microglia and linked to retinal neovascularization. **(A)** Immunofluorescence staining of retinal sections shows colocalization of HMOX1 with microglia (Iba1) and endothelial cells (IB4). **(B–C)** Quantification of Iba1$^+$ microglia and IB4$^+$ endothelial cells in OIR and control retinas (n = 6). **(D)** Whole-mount immunostaining shows colocalization of HMOX1 with microglia and endothelial cells. **(E)** qPCR analysis of HMOX1 mRNA in CON and OIR retinas across P7–P25 (n = 5). **(F–G)** Western blot and quantification of HMOX1 protein expression at P7–P25 (n = 4). **(H–I)** Western blot and quantification of HMOX1 protein in HMC3 cells in control and hypoxia groups (12 H, 24 H, 48 H) (n = 3). **(J)** qPCR showing HMOX1 mRNA levels in HMC3 cells under hypoxia (n = 3). **(K–L)** Immunofluorescence staining showing increased HMOX1 expression in HMC3 under hypoxia (n = 6). Scale bars: 50 μm in (A), 100 μm in (D), and (K). *P < 0.05; **P < 0.01; ***P < 0.001; ****P < 0.0001.



(caption on next page)

Fig. 4. Microglia-specific deletion of HMOX1 alleviates neovascularization in OIR mice. **(A)** Schematic diagram and representative images of the OIR model. **(B–C)** Western blot analysis confirming efficient knockout of HMOX1 in HMOX1 cKO ($HMOX1^{fl/fl}$; $Cx3cr1\text{-}CreERT2^{+/-}$) mice compared to $HMOX1^{fl/fl}$ mice (n = 3). **(D)** Immunofluorescence staining of OIR retinas showing co-localization of HMOX1 with microglia (Iba1) and endothelial cells (IB4). **(E–G)** Quantification of microglia (Iba1), neovascular area (IB4), and HMOX1 levels in $HMOX1^{fl/fl}$ and HMOX1 cKO groups under OIR (n = 6). **(H)** Representative OCT and fundus images across CON-$HMOX1^{fl/fl}$, CON-cKO, OIR-$HMOX1^{fl/fl}$, and OIR-cKO groups. **(I–J)** Quantification of total and inner retinal thickness from OCT images (n = 6). **(K)** Whole-mount staining of retinas showing neovascular and avascular areas in the four groups. **(L–M)** Quantification of neovascular and avascular areas (n = 6). **(N)** H&E staining showing retinal morphology and preretinal neovascular numbers. **(O–P)** Quantification of total retinal thickness and preretinal neovascular nuclei based on H&E-stained sections (n = 6). Scale bars: 50 μm in (D) and (N), 100 μm in (H), 500 μm in (K). *P < 0.05; **P < 0.01; ***P < 0.001; ****P < 0.0001.

limited knockdown efficiency of HMOX1 siRNAs in HMC3 cells, pharmacological inhibition was adopted using ZnPP, a selective HMOX1 inhibitor [19]. MTT assays confirmed that ZnPP at 10 and 20 μM was non-toxic to HMC3 cells (Fig. S2D), and both concentrations effectively suppressed HMOX1 expression (Fig. S2E–F). Based on these results, 10 μM ZnPP was selected for subsequent experiments.

HRMVECs were co-cultured with HMC3 cells under normoxic or hypoxic conditions, with or without ZnPP, forming four experimental groups: control, control + ZnPP, hypoxia, and hypoxia + ZnPP. EdU incorporation assays revealed a significant reduction in endothelial proliferation upon ZnPP treatment under hypoxia (Fig. 5A and B). Similarly, wound healing and transwell migration assays showed impaired HRMVEC migratory capacity in the hypoxia + ZnPP group compared to hypoxia alone (Fig. 5C–F). In addition, Matrigel tube formation assays demonstrated that HMOX1 inhibition in microglia markedly attenuated the pro-angiogenic phenotype of endothelial cells (Fig. 5G and H). Together, these results suggest that microglial HMOX1 enhances endothelial angiogenic activity in hypoxic conditions and may play a critical role in mediating microglia–endothelial crosstalk during retinal neovascularization.

3.6. Inhibition of microglial HMOX1 suppresses retinal neovascularization via downregulation of endothelial STAT3

Immunofluorescence staining of retinal tissues from four groups—normoxic $HMOX1^{fl/fl}$ controls (CON-$HMOX1^{fl/fl}$), normoxic microglia-specific HMOX1 conditional knockout (CON-cKO), OIR $HMOX1^{fl/fl}$ controls (OIR-$HMOX1^{fl/fl}$), and OIR microglia-specific HMOX1 conditional knockout (OIR-cKO)—revealed STAT3 expression was markedly reduced, and this was accompanied by a significant decrease in neovascular cell formation (Fig. 6A–C). To further investigate the temporal dynamics of key angiogenic molecules, Western blot analyses were performed on retinal lysates collected at P7, P12, P17, and P25. The expression of pSTAT3, STAT3, HMOX1, and VEGF peaked at

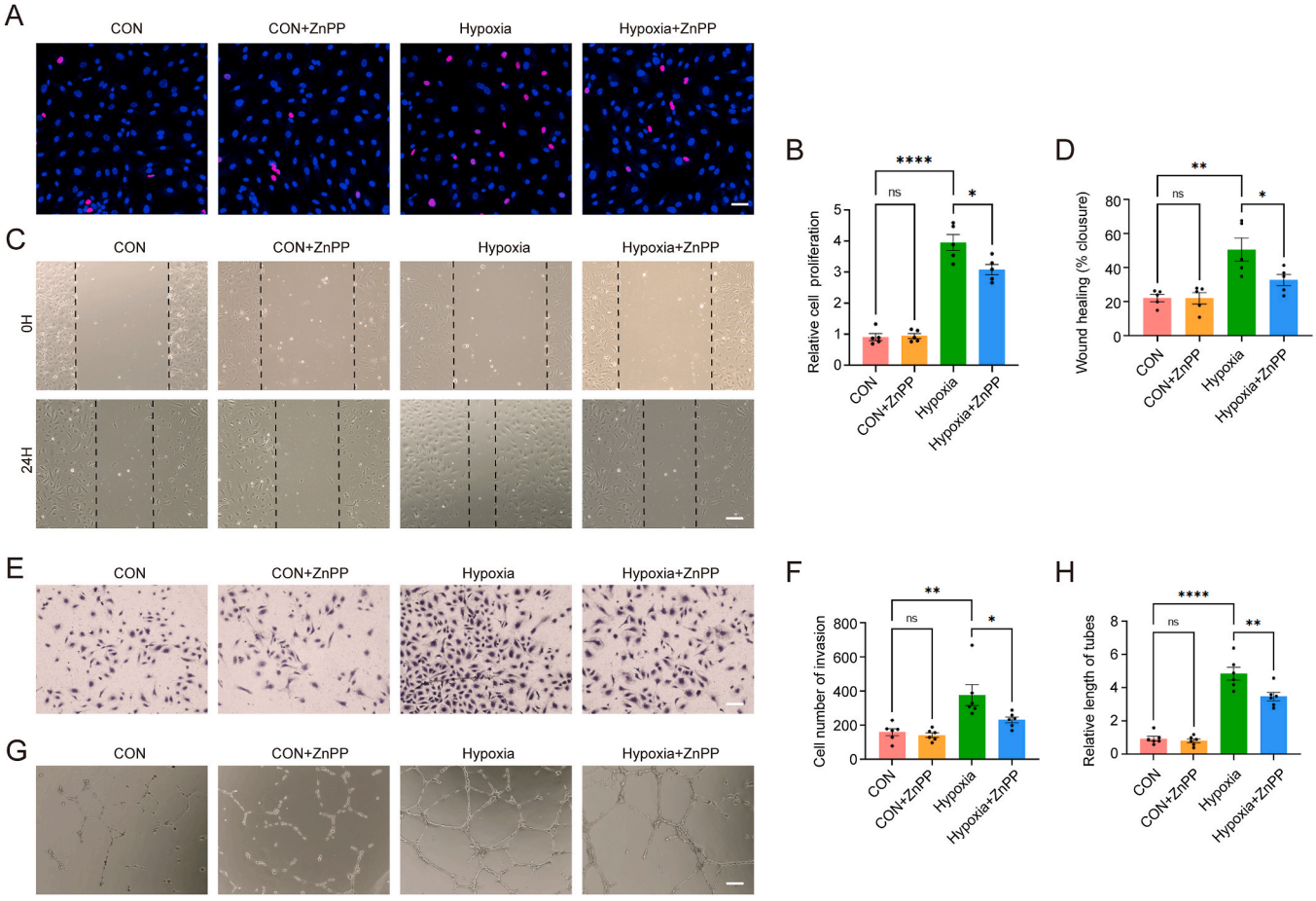


Fig. 5. Inhibition of microglial HMOX1 suppresses endothelial angiogenic activities in vitro. **(A–B)** EdU assay and quantification of HRMVEC proliferation in co-culture with HMC3 cells in four groups: Control, Control + ZnPP, Hypoxia, and Hypoxia + ZnPP (n = 6). **(C–D)** Wound healing assay showing HRMVEC migration and corresponding quantification across groups (n = 6). **(E–F)** Transwell migration assay and quantification of HRMVECs under indicated conditions (n = 6). **(G–H)** Tube formation assay demonstrating endothelial angiogenic capacity and quantification of tube structures (n = 6). Scale bars: 50 μm in (A),250 μm in (C), (E), and (G). *P < 0.05; **P < 0.01; ****P < 0.0001.

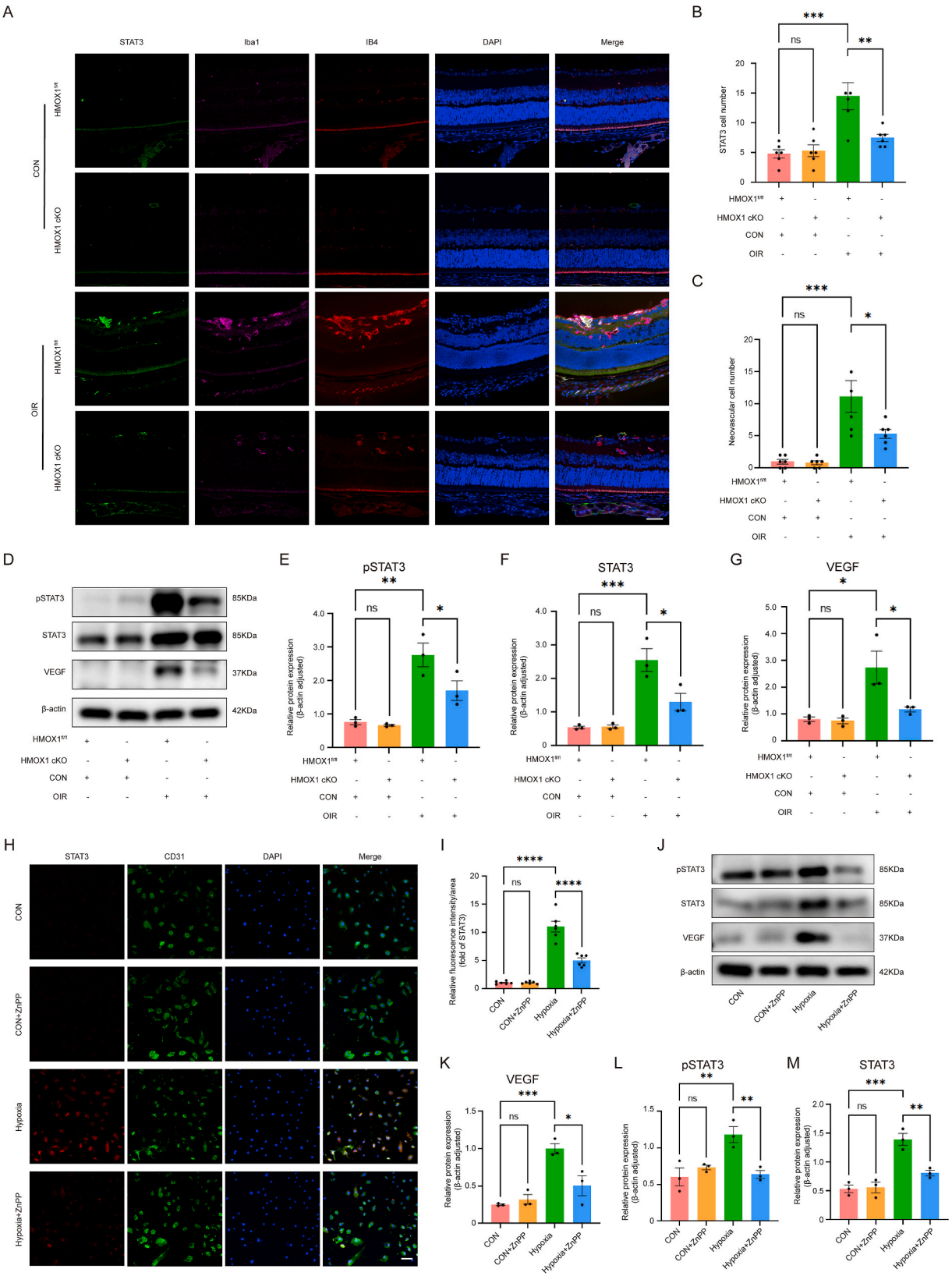


Fig. 6. Microglial HMOX1 regulates retinal neovascularization via endothelial STAT3 activation. **(A)** Immunofluorescence staining of retinal sections showing co-localization of STAT3 with Iba1$^+$ microglia and IB4$^+$ endothelial cells in CON-HMOX1$^{fl/fl}$, CON-cKO, OIR-HMOX1$^{fl/fl}$, and OIR-cKO groups. **(B–C)** Quantification of STAT3 expression and preretinal neovascular nuclei in retinal sections (n = 6). **(D)** Western blot analysis of STAT3, pSTAT3, and VEGF expression in retinas from the four groups at P17. **(E–G)** Densitometric quantification of pSTAT3, total STAT3, and VEGF levels from (D) (n = 3). **(H–I)** Immunofluorescence staining and quantification of pSTAT3 in CD31$^+$ endothelial cells under hypoxia with/without ZnPP treatment (n = 6). **(J–M)** Western blot and densitometric analysis of pSTAT3, STAT3, and VEGF in co-cultured HRMVECs (n = 3). *Scale bars: 50 μm in (A), 100 μm in (H). *P < 0.05; **P < 0.01; ***P < 0.001; ****P < 0.0001.

P17 in the OIR group, consistent with the neovascularization apex of the model (Fig. S6A–E). All proteins were significantly downregulated in OIR-cKO mice compared to OIR-HMOX1$^{fl/fl}$ controls, confirming the involvement of HMOX1 in modulating angiogenic signaling (Fig. 6D–G).

These findings were further validated in vitro. Under hypoxic conditions, immunofluorescence staining revealed decreased STAT3 expression in CD31^{+} endothelial cells co-cultured with ZnPP-treated microglia (Fig. 6H and I). Consistently, Western blotting showed that ZnPP suppressed the hypoxia-induced upregulation of pSTAT3, total STAT3, and VEGF in endothelial cells, with no significant changes observed under control (Fig. 6J–M). Together, these results indicate that microglial HMOX1 promotes retinal angiogenesis, by enhancing STAT3–VEGF signaling in endothelial cells. To ensure transparency, the original uncropped Western blot images corresponding to all figures are provided in supplementary information (Fig. S7).

4. Discussion

Retinal neovascularization is a hallmark of ischemia-related retinal diseases such as ROP. However, current interventions for ROP are typically implemented after disease onset and often result in suboptimal outcomes [20,21]. The limited efficacy of anti-VEGF therapies in a subset of patients suggests the involvement of additional angiogenic regulators beyond VEGF alone [22]. In this study, we identified HMOX1 as a key modulator of hypoxia-induced retinal neovascularization, acting predominantly through activation of the endothelial STAT3–VEGF signaling axis. Microglia-specific conditional knockout of HMOX1 in the OIR model significantly attenuated pathological angiogenesis, accompanied by a marked reduction in STAT3 and VEGF expression, underscoring the central role of microglial HMOX1 in hypoxia-driven vascular remodeling. Furthermore, in a hypoxia-induced microglia–endothelial co-culture system, inhibition of HMOX1 in microglia led to reduced endothelial proliferation and migration, as well as decreased STAT3 activation and VEGF expression. Together, these findings highlight microglial HMOX1 as an upstream regulator of angiogenic signaling and a promising therapeutic target for ROP and other retinal neovascular disorders.

Although the OIR rat model exhibits delayed peripheral vascular development that more closely resembles the spatial distribution of neovascularization in human ROP, the mouse OIR model remains the most widely adopted experimental system for mechanistic studies [23,24]. Compared with rats, mice offer higher genetic accessibility, well-established transgenic tools, and reproducible vascular responses, making them particularly suitable for dissecting cell type–specific pathways. To investigate the molecular mechanisms underlying retinal neovascularization in ROP, we integrated bulk RNA-seq and scRNA-seq analyses from the OIR model. Bulk RNA-seq revealed significant upregulation of HMOX1 in OIR retinas, with expression dynamics closely paralleling the temporal progression of pathological neovascularization, suggesting a potential regulatory role in angiogenesis. HMOX1 is known to be elevated in hypoxia-associated diseases, including age-related macular degeneration and various cancers, where it contributes to neovascularization [25–27], implicating its relevance in OIR. scRNA-seq further demonstrated that HMOX1 expression is enriched specifically in microglia. As the primary immune cells in the retina, microglia are increasingly recognized as key modulators of angiogenesis through their response to hypoxic stress [6,28,29]. Previous studies have shown that HMOX1 facilitates M2 macrophage polarization and regulates inflammation in hypoxia-driven pathologies such as portal hypertension [16,30,31], supporting its role as a stress-responsive mediator in microglia. Together, these findings suggest that microglial HMOX1 contributes to pathological angiogenesis by modulating the retinal hypoxic microenvironment. Notably, this study is the first to characterize HMOX1^{+} microglia in the OIR retina and to delineate their distinct transcriptional profile.

Studies have demonstrated that microglia play a pivotal role in neovascularization within both the central nervous system and the retina [32–34]. Under hypoxic conditions, these cells are recruited to neovascular regions and often reside in close proximity to endothelial cells, implicating their involvement in local vascular remodeling [33,35–37]. While their proangiogenic effects are well established [38–40], the mechanisms by which microglia directly interact with nascent endothelial structures, especially under hypoxia, remain incompletely understood. In this study, bulk and single-cell RNA sequencing indicated that microglia may contribute to retinal neovascularization through paracrine communication with neighboring endothelial cells. In the OIR model, HMOX1 was specifically upregulated in microglia, with its spatial distribution overlapping neovascular regions, suggesting a potential mediating role. Conditional knockout of HMOX1 in microglia resulted in reduced microglial accumulation and diminished endothelial proliferation. Complementary in vitro assays confirmed that HMOX1 inhibition in microglia impaired endothelial proliferation and migration, supporting a direct functional interaction. Collectively, these findings suggest that microglial HMOX1 drives hypoxia-induced retinal neovascularization through intercellular signaling. Beyond establishing HMOX1 as a key effector, this study delineates the spatiotemporal pattern of microglial recruitment, activation, and angiogenic action. It also highlights the importance of immune–vascular crosstalk in retinal pathology. Future research should further explore the downstream effectors of HMOX1^{+} microglia and their therapeutic potential in conditions such as ROP.

HMOX1 is a well-recognized cytoprotective enzyme with antioxidant, anti-inflammatory, and pro-angiogenic functions [41], emerging evidence suggests that sustained HMOX1 activation under pathological conditions may paradoxically induce cytotoxicity and drive abnormal angiogenesis [42]. Prior studies have shown that HMOX1 can stimulate VEGF expression and promote vascular proliferation [19,43]. In our study, HMOX1 expression in the OIR retina closely mirrored the temporal progression of neovascularization. Both in vivo conditional knockout and pharmacological inhibition using ZnPP significantly suppressed VEGF expression and attenuated neovascularization, consistent with previous reports [16,44,45]. In agreement with earlier findings, these effects were accompanied by reduced STAT3 signaling, supporting a mechanism by which HMOX1 may promote angiogenesis via STAT3 activation [46,47].

Supporting this, PPI network analysis of HMOX1^{+} microglia revealed strong interconnectivity with angiogenesis-related regulators including STAT3 and VEGF. CellChat analysis further showed enhanced ligand–receptor interactions between microglia and endothelial cells, particularly through the VEGFA–VEGFR2 axis [48,49], suggesting that HMOX1^{+} microglia may modulate endothelial behavior via paracrine signaling [50,51]. Both in vitro and in vivo, HMOX1 inhibition resulted in reduced STAT3 expression, accompanied by a concomitant decrease in VEGF. These findings suggest that HMOX1 functions as an upstream modulator of STAT3, thereby contributing to VEGF-driven neovascularization. Together, these results propose a hypoxia–microglia–endothelium signaling axis, in which hypoxia-induced HMOX1 upregulation in microglia activates downstream STAT3–VEGF signaling and augments microglia–endothelial communication, ultimately driving angiogenesis. This mechanistic insight highlights HMOX1 as a potential molecular target for ROP and other hypoxia-related retinal vascular diseases. Further supporting this hypothesis, previous studies have shown that HMOX1 overexpression enhances STAT3 phosphorylation and transcriptional activity. These effects contribute to anti-inflammatory and cytoprotective responses in hepatic tissues, where STAT3 acts as a key downstream effector of HMOX1 signaling [52]. Moreover, HMOX1 has been shown to activate STAT3 signaling to promote tumor cell proliferation and is recognized as an upstream regulator of STAT3 in various disease contexts [53]. Conversely, STAT3 activation can also induce HMOX1 expression, forming a positive feedback loop that suppresses inflammation [54]. Taken together, these findings highlight a complex bidirectional

regulatory relationship between HMOX1 and STAT3. Taken together, our study expands current understanding of HMOX1 signaling and supports its potential as a therapeutic target in retinal vascular diseases. In summary, our findings delineate a novel HMOX1–STAT3–VEGF signaling cascade that contributes to retinal neovascularization. This microglia-mediated axis provides mechanistic insight into hypoxia-induced vascular remodeling and offers promising molecular targets for early intervention in retinopathy of prematurity and other ischemia-related retinal vascular diseases.

Although this study elucidates the critical role of microglial HMOX1 in retinal neovascularization and reveals its interaction with adjacent endothelial cells, several limitations should be acknowledged. First, the downstream signaling mechanisms of HMOX1 require further clarification. While our STAT3 inhibition experiments provide preliminary evidence of its involvement, it remains uncertain whether STAT3 is the primary effector or part of a broader signaling network. Transcriptomic and protein–protein interaction analyses suggest additional candidates such as hypoxia-inducible factor 2-alpha (HIF-2α) and early growth response 2 (Egr2), warranting more comprehensive pathway mapping. Second, the absence of validation using clinical samples from patients with ROP limits translational relevance. Future studies should consider incorporating patient-derived samples—such as blood, tear fluid, or aqueous humor—to enable validation across RNA, protein, and metabolite levels.

Although this study centers on ROP, the OIR model serves as a representative paradigm of ischemia-induced retinal neovascularization. The mechanistic insights uncovered here may therefore be broadly applicable to other retinal vascular disorders, such as diabetic retinopathy and retinal vein occlusion, where hypoxia and oxidative stress act as common pathogenic drivers.

5. Conclusions

In conclusion, this study demonstrates that microglial HMOX1 plays a critical role in retinal angiogenesis. HMOX1 expression is markedly induced in microglia under hypoxic conditions and spatiotemporally associated with pathological vascular growth. Mechanistically, microglial HMOX1 modulates endothelial STAT3 activation and VEGF production, thereby promoting angiogenic progression. These findings identify a microglia–endothelium signaling axis mediated by HMOX1 and provide mechanistic insight into the immune regulation of pathological angiogenesis in ischemia-related retinal diseases such as ROP, as well as other hypoxia-driven neovascular disorders.

CRediT authorship contribution statement

Yaling Liu: Writing – review & editing, Writing – original draft, Methodology, Investigation, Formal analysis, Conceptualization. **Jiannan Tang:** Writing – original draft, Formal analysis. **Peiling Wei:** Methodology. **Zhen Yu:** Supervision, Methodology. **Zhifei Wu:** Methodology. **Xinyu Zhao:** Formal analysis. **Hui Qi:** Methodology. **Ping Liu:** Methodology. **Mianying Zheng:** Data curation. **Shengli Mi:** Data curation. **Wei Du:** Methodology. **Demetrios G. Vavvas:** Supervision, Methodology. **Kaixuan Cui:** Supervision, Methodology. **Guoming Zhang:** Supervision, Methodology.

Ethics approval and consent to participate

This study was approved by the Ethics Committee of Shenzhen Eye Hospital (Approval No. D2307020). All institutions abided by the tenets of the Declaration of Helsinki.

Consent for publication

Not applicable.

Availability of data and materials

Data are available from the first author upon reasonable request.

Financial support

National Natural Science Foundation of China (82271103, 82401272, 82301226, 82401315), Shenzhen Medical Research Fund (C2301005, C2501034, A2403020), Sanming Project of Medicine in Shenzhen (SZSM202311018), Guangdong Provincial Medical Research Fund Project (B2025169), Guangdong Basic and Applied Basic Research Foundation (2022A1515110865), Shenzhen Science and Technology R&D Fund Project (JCYJ20220530153607015, JCYJ2024081315 2703005), China Ophthalmology New Technology Incubation Project.

Conflict of interest statement

The authors declare that there is no conflict of interest regarding the publication of this manuscript.

Acknowledgements

Not applicable.

Abbreviations

ANOVA	one-way analysis of variance
CON	Control
Cx3cr1-Cre	Cx3cr1 promoter-driven Cre recombinase
ECL	Enhanced chemiluminescence
Ecs	endothelial cells
EdU	Enhanced chemiluminescence
Egr2	early growth response 2
FFA	Fundus fluorescein angiography
GO	Gene Ontology
HMC3	human microglial cell line
HMOX1	heme oxygenase-1
HIF-2α	hypoxia-inducible factor 2-alpha
HRMVECs	human retinal microvascular endothelial cells
IB4	Isolectin B4
KEGG	Kyoto Encyclopedia of Genes and Genomes
MTT	3-(4,5-dimethylthiazol-2-yl)-2,5-diphenyl tetrazolium bromide
OCT	Optical coherence tomography
OIR	oxygen-induced retinopathy
PFA	paraformaldehyde
PPI	protein–protein interaction
Qpcr	Quantitative PCR
ROP	Retinopathy of prematurity
scRNA-seq	single-cell RNA sequencing
STAT3	signal transducer and activator of transcription 3
UMAP	Uniform Manifold Approximation and Projection
VEGF	vascular endothelial growth factor
ZnPP	zinc protoporphyrin IX

Appendix A. Supplementary data

Supplementary data to this article can be found online at https://doi.org/10.1016/j.freeradbiomed.2025.11.018.

References

[1] C. Gilbert, J. Rahi, M. Eckstein, J. O'Sullivan, A. Foster, Retinopathy of prematurity in middle-income countries, Lancet 350 (9070) (1997) 12–14, https://doi.org/10.1016/S0140-6736(97)01107-0.

[2] A. Hellstrom, L.E. Smith, O. Dammann, Retinopathy of prematurity, Lancet 382 (9902) (2013) 1445–1457, https://doi.org/10.1016/S0140-6736(13)60178-6.

[3] B. Jasani, R. Nanavati, N. Kabra, Mechanisms and management of retinopathy of prematurity, N. Engl. J. Med. 368 (12) (2013) 1161–1162, https://doi.org/10.1056/NEJMc1301021.
[4] T. Chan-Ling, G.A. Gole, G.E. Quinn, S.J. Adamson, B.A. Darlow, Pathophysiology, screening and treatment of ROP: a multi-disciplinary perspective, Prog. Retin. Eye Res. 62 (2018) 77–119, https://doi.org/10.1016/j.preteyeres.2017.09.002.
[5] A.S. Tsai, H.D. Chou, X.C. Ling, T. Al-Khaled, N. Valikodath, E. Cole, et al., Assessment and management of retinopathy of prematurity in the era of anti-vascular endothelial growth factor (VEGF), Prog. Retin. Eye Res. 88 (2022) 101018, https://doi.org/10.1016/j.preteyeres.2021.101018.
[6] C. He, Y. Liu, Z. Huang, Z. Yang, T. Zhou, S. Liu, et al., A specific RIP3(+) subpopulation of microglia promotes retinopathy through a hypoxia-triggered necroptotic mechanism, Proc. Natl. Acad. Sci. U. S. A. 118 (11) (2021), https://doi.org/10.1073/pnas.2023290118.
[7] N. Dudvarski Stankovic, M. Teodorczyk, R. Ploen, F. Zipp, M.H.H. Schmidt, Microglia-blood vessel interactions: a double-edged sword in brain pathologies, Acta Neuropathol. 131 (3) (2016) 347–363, https://doi.org/10.1007/s00401-015-1524-y.
[8] F. Binet, G. Cagnone, S. Crespo-Garcia, M. Hata, M. Neault, A. Dejda, et al., Neutrophil extracellular traps target senescent vasculature for tissue remodeling in retinopathy, Science 369 (6506) (2020), https://doi.org/10.1126/science.aay5356.
[9] Z. Liu, H. Shi, J. Xu, Q. Yang, Q. Ma, X. Mao, et al., Single-cell transcriptome analyses reveal microglia types associated with proliferative retinopathy, JCI Insight 7 (23) (2022), https://doi.org/10.1172/jci.insight.160940.
[10] Y. Li, X. He, R. Kawaguchi, Y. Zhang, Q. Wang, A. Monavarfeshani, et al., Microglia-organized scar-free spinal cord repair in neonatal mice, Nature 587 (7835) (2020) 613–618, https://doi.org/10.1038/s41586-020-2795-6.
[11] E.M. Sikorski, T. Hock, N. Hill-Kapturczak, A. Agarwal, The story so far: molecular regulation of the heme oxygenase-1 gene in renal injury, Am. J. Physiol. Ren. Physiol. 286 (3) (2004) F425–F441, https://doi.org/10.1152/ajprenal.00297.2003.
[12] A.C. Zenclussen, A. Sollwedel, A.Z. Bertoja, K. Gerlof, M.L. Zenclussen, C. Woiciechowsky, et al., Heme oxygenase as a therapeutic target in immunological pregnancy complications, Int. Immunopharmacol. 5 (1) (2005) 41–51, https://doi.org/10.1016/j.intimp.2004.09.011.
[13] Y. Miyata, S. Kanda, K. Mitsunari, A. Asai, H. Sakai, Heme oxygenase-1 expression is associated with tumor aggressiveness and outcomes in patients with bladder cancer: a correlation with smoking intensity, Transl. Res. 164 (6) (2014) 468–476, https://doi.org/10.1016/j.trsl.2014.06.010.
[14] J. Dulak, A. Loboda, A. Zagorska, A. Jozkowicz, Complex role of heme oxygenase-1 in angiogenesis, Antioxidants Redox Signal. 6 (5) (2004) 858–866, https://doi.org/10.1089/ars.2004.6.858.
[15] A. Jozkowicz, I. Huk, A. Nigisch, G. Weigel, W. Dietrich, R. Motterlini, et al., Heme oxygenase and angiogenic activity of endothelial cells: stimulation by carbon monoxide and inhibition by tin protoporphyrin-IX, Antioxidants Redox Signal. 5 (2) (2003) 155–162, https://doi.org/10.1089/152308603764816514.
[16] B. Bussolati, A. Ahmed, H. Pemberton, R.C. Landis, F. Di Carlo, D.O. Haskard, et al., Bifunctional role for VEGF-induced heme oxygenase-1 in vivo: induction of angiogenesis and inhibition of leukocytic infiltration, Blood 103 (3) (2004) 761–766, https://doi.org/10.1182/blood-2003-06-1974.
[17] K.M. Connor, N.M. Krah, R.J. Dennison, C.M. Aderman, J. Chen, K.I. Guerin, et al., Quantification of oxygen-induced retinopathy in the mouse: a model of vessel loss, vessel regrowth and pathological angiogenesis, Nat. Protoc. 4 (11) (2009) 1565–1573, https://doi.org/10.1038/nprot.2009.187.
[18] L.E. Smith, E. Wesolowski, A. McLellan, S.K. Kostyk, R. D'Amato, R. Sullivan, et al., Oxygen-induced retinopathy in the mouse, Investig. Ophthalmol. Vis. Sci. 35 (1) (1994) 101–111.
[19] C.C. Cheng, S.S. Guan, H.J. Yang, C.C. Chang, T.Y. Luo, J. Chang, et al., Blocking heme oxygenase-1 by zinc protoporphyrin reduces tumor hypoxia-mediated VEGF release and inhibits tumor angiogenesis as a potential therapeutic agent against colorectal cancer, J. Biomed. Sci. 23 (2016) 18, https://doi.org/10.1186/s12929-016-0219-6.
[20] D.K. VanderVeen, M. Melia, M.B. Yang, A.K. Hutchinson, L.B. Wilson, S. R. Lambert, Anti-vascular endothelial growth factor therapy for primary treatment of type 1 retinopathy of prematurity: a report by the American academy of ophthalmology, Ophthalmology 124 (5) (2017) 619–633, https://doi.org/10.1016/j.ophtha.2016.12.025.
[21] A. Stahl, T.U. Krohne, N. Eter, I. Oberacher-Velten, R. Guthoff, S. Meltendorf, et al., Comparing alternative ranibizumab dosages for safety and efficacy in retinopathy of prematurity: a randomized clinical trial, JAMA Pediatr. 172 (3) (2018) 278–286, https://doi.org/10.1001/jamapediatrics.2017.4838.
[22] S. Yang, J. Zhao, X. Sun, Resistance to anti-VEGF therapy in neovascular age-related macular degeneration: a comprehensive review, Drug Des. Dev. Ther. 10 (2016) 1857–1867, https://doi.org/10.2147/DDDT.S97653.
[23] C.B. Kim, P.A. D'Amore, K.M. Connor, Revisiting the mouse model of oxygen-induced retinopathy, Eye Brain 8 (2016) 67–79, https://doi.org/10.2147/EB.S94447.
[24] A. Scott, M. Fruttiger, Oxygen-induced retinopathy: a model for vascular pathology in the retina, Eye (Lond) 24 (3) (2010) 416–421, https://doi.org/10.1038/eye.2009.306.
[25] V. Consoli, V. Sorrenti, V. Pittala, K. Greish, A.G. D'Amico, G. Romeo, et al., Heme oxygenase modulation drives ferroptosis in TNBC cells, Int. J. Mol. Sci. 23 (10) (2022), https://doi.org/10.3390/ijms23105709.
[26] D. Yan, J. Xu, X. Wang, J. Zhang, G. Zhao, Y. Lin, et al., Spiro-oxindole skeleton compounds are efficient inhibitors for indoleamine 2,3-Dioxygenase 1: an attractive target for tumor immunotherapy, Int. J. Mol. Sci. 23 (9) (2022), https://doi.org/10.3390/ijms23094668.
[27] K. Skrzypek, M. Tertil, S. Golda, M. Ciesla, K. Weglarczyk, G. Collet, et al., Interplay between heme oxygenase-1 and miR-378 affects non-small cell lung carcinoma growth, vascularization, and metastasis, Antioxidants Redox Signal. 19 (7) (2013) 644–660, https://doi.org/10.1089/ars.2013.5184.
[28] J. Li, S. Yu, X. Lu, K. Cui, X. Tang, Y. Xu, et al., The phase changes of M1/M2 phenotype of microglia/macrophage following oxygen-induced retinopathy in mice, Inflamm. Res. 70 (2) (2021) 183–192, https://doi.org/10.1007/s00011-020-01427-w.
[29] X. Wang, W. Fan, N. Li, Y. Ma, M. Yao, G. Wang, et al., YY1 lactylation in microglia promotes angiogenesis through transcription activation-mediated upregulation of FGF2, Genome Biol. 24 (1) (2023) 87, https://doi.org/10.1186/s13059-023-02931-y.
[30] B. Angermayr, M. Mejias, J. Gracia-Sancho, J.C. Garcia-Pagan, J. Bosch, M. Fernandez, Heme oxygenase attenuates oxidative stress and inflammation, and increases VEGF expression in portal hypertensive rats, J. Hepatol. 44 (6) (2006) 1033–1039, https://doi.org/10.1016/j.jhep.2005.09.021.
[31] W. Sha, B. Zhao, H. Wei, Y. Yang, H. Yin, J. Gao, et al., Astragalus polysaccharide ameliorates vascular endothelial dysfunction by stimulating macrophage M2 polarization via potentiating Nrf2/HO-1 signaling pathway, Phytomedicine 112 (2023) 154667, https://doi.org/10.1016/j.phymed.2023.154667.
[32] A. Uemura, M. Fruttiger, P.A. D'Amore, S. De Falco, A.M. Joussen, F. Sennlaub, et al., VEGFR1 signaling in retinal angiogenesis and microinflammation, Prog. Retin. Eye Res. 84 (2021) 100954, https://doi.org/10.1016/j.preteyeres.2021.100954.
[33] Z. Liu, J. Xu, Q. Ma, X. Zhang, Q. Yang, L. Wang, et al., Glycolysis links reciprocal activation of myeloid cells and endothelial cells in the retinal angiogenic niche, Sci. Transl. Med. 12 (555) (2020), https://doi.org/10.1126/scitranslmed.aay1371.
[34] Z. Li, J. Xiao, X. Xu, W. Li, R. Zhong, L. Qi, et al., M-CSF, IL-6, and TGF-Beta promote generation of a new subset of tissue repair macrophage for traumatic brain injury recovery, Sci. Adv. 7 (11) (2021), https://doi.org/10.1126/sciadv.abb6260.
[35] W. Fan, W. Huang, J. Chen, N. Li, L. Mao, S. Hou, Retinal microglia: functions and diseases, Immunology 166 (3) (2022) 268–286, https://doi.org/10.1111/imm.13479.
[36] A.D. Umpierre, L.J. Wu, How microglia sense and regulate neuronal activity, Glia 69 (7) (2021) 1637–1653, https://doi.org/10.1002/glia.23961.
[37] S.C. Huang, A.M. Smith, B. Everts, M. Colonna, E.L. Pearce, J.D. Schilling, et al., Metabolic reprogramming mediated by the mTORC2-IRF4 signaling axis is essential for macrophage alternative activation, Immunity 45 (4) (2016) 817–830, https://doi.org/10.1016/j.immuni.2016.09.016.
[38] S.P. Kambhampati, I.A. Bhutto, T. Wu, K. Ho, D.S. McLeod, G.A. Lutty, et al., Systemic dendrimer nanotherapies for targeted suppression of choroidal inflammation and neovascularization in age-related macular degeneration, J. Contr. Release 335 (2021) 527–540, https://doi.org/10.1016/j.jconrel.2021.05.035.
[39] Q. Jin, J. Cheng, Y. Liu, J. Wu, X. Wang, S. Wei, et al., Improvement of functional recovery by chronic metformin treatment is associated with enhanced alternative activation of microglia/macrophages and increased angiogenesis and neurogenesis following experimental stroke, Brain Behav. Immun. 40 (2014) 131–142, https://doi.org/10.1016/j.bbi.2014.03.003.
[40] S. Brandenburg, A. Muller, K. Turkowski, Y.T. Radev, S. Rot, C. Schmidt, et al., Resident microglia rather than peripheral macrophages promote vascularization in brain tumors and are source of alternative pro-angiogenic factors, Acta Neuropathol. 131 (3) (2016) 365–378, https://doi.org/10.1007/s00401-015-1529-6.
[41] B. Bussolati, J.C. Mason, Dual role of VEGF-induced heme-oxygenase-1 in angiogenesis, Antioxidants Redox Signal. 8 (7–8) (2006) 1153–1163, https://doi.org/10.1089/ars.2006.8.1153.
[42] M. Ferrando, G. Gueron, B. Elguero, J. Giudice, A. Salles, F.C. Leskow, et al., Heme oxygenase 1 (HO-1) challenges the angiogenic switch in prostate cancer, Angiogenesis 14 (4) (2011) 467–479, https://doi.org/10.1007/s10456-011-9230-4.
[43] G. Chen, J. Long, Y. Zhang, X. Zhou, B. Gao, Z. Qin, et al., Fascia-derived stem cells enhance fat graft retention by promoting vascularization through the HMOX1-HIF-1alpha pathway, Stem Cell Res. Ther. 16 (1) (2025) 92, https://doi.org/10.1186/s13287-025-04204-w.
[44] J. Cisowski, A. Loboda, A. Jozkowicz, S. Chen, A. Agarwal, J. Dulak, Role of heme oxygenase-1 in hydrogen peroxide-induced VEGF synthesis: effect of HO-1 knockout, Biochem. Biophys. Res. Commun. 326 (3) (2005) 670–676, https://doi.org/10.1016/j.bbrc.2004.11.083.
[45] H. Maamoun, M. Zachariah, J.H. McVey, F.R. Green, A. Agouni, Heme oxygenase (HO)-1 induction prevents endoplasmic reticulum stress-mediated endothelial cell death and impaired angiogenic capacity, Biochem. Pharmacol. 127 (2017) 46–59, https://doi.org/10.1016/j.bcp.2016.12.009.
[46] M.L. Ji, J.N. Wang, M.F. Wu, C.H. Xu, M.M. Zhang, W.B. Chang, et al., Targeting Stat3 with conditional knockout or PROTAC technology alleviates renal injury by limiting pyroptosis, EBioMedicine 116 (2025) 105739, https://doi.org/10.1016/j.ebiom.2025.105739.
[47] J. Zhou, K. Tison, H. Zhou, L. Bai, R.K. Acharyya, D. McEachern, et al., STAT5 and STAT3 balance shapes dendritic cell function and tumour immunity, Nature (2025), https://doi.org/10.1038/s41586-025-09000-3.
[48] L. Chen, X. Xie, T. Wang, L. Xu, Z. Zhai, H. Wu, et al., ARL13B promotes angiogenesis and glioma growth by activating VEGFA-VEGFR2 signaling, Neuro Oncol. 25 (5) (2023) 871–885, https://doi.org/10.1093/neuonc/noac245.

[49] G. Mastrella, M. Hou, M. Li, V.M. Stoecklein, N. Zdouc, M.N.M. Volmar, et al., Targeting APLN/APLNR improves antiangiogenic efficiency and blunts proinvasive side effects of VEGFA/VEGFR2 blockade in glioblastoma, Cancer Res. 79 (9) (2019) 2298–2313, https://doi.org/10.1158/0008-5472.CAN-18-0881.

[50] M. Neunlist, L. Van Landeghem, M.M. Mahe, P. Derkinderen, S.B. des Varannes, M. Rolli-Derkinderen, The digestive neuronal-glial-epithelial unit: a new actor in gut health and disease, Nat. Rev. Gastroenterol. Hepatol. 10 (2) (2013) 90–100, https://doi.org/10.1038/nrgastro.2012.221.

[51] M. Kioko, S. Mwangi, A. Pance, L.I. Ochola-Oyier, S. Kariuki, C. Newton, et al., The mRNA content of plasma extracellular vesicles provides a window into molecular processes in the brain during cerebral malaria, Sci. Adv. 10 (33) (2024) eadl2256, https://doi.org/10.1126/sciadv.adl2256.

[52] B. Ke, X.D. Shen, H. Ji, N. Kamo, F. Gao, M.C. Freitas, et al., HO-1-STAT3 axis in mouse liver ischemia/reperfusion injury: regulation of TLR4 innate responses through PI3K/PTEN signaling, J. Hepatol. 56 (2) (2012) 359–366, https://doi.org/10.1016/j.jhep.2011.05.023.

[53] J. Song, X. Zhang, Z. Liao, H. Liang, L. Chu, W. Dong, et al., 14-3-3zeta inhibits heme oxygenase-1 (HO-1) degradation and promotes hepatocellular carcinoma proliferation: involvement of STAT3 signaling, J. Exp. Clin. Cancer Res. 38 (1) (2019) 3, https://doi.org/10.1186/s13046-018-1007-9.

[54] P. Mandal, P.H. Park, M.R. McMullen, B.T. Pratt, L.E. Nagy, The anti-inflammatory effects of adiponectin are mediated via a heme oxygenase-1-dependent pathway in rat kupffer cells, Hepatology 51 (4) (2010) 1420–1429, https://doi.org/10.1002/hep.23427.